24th International Conference on Renewable Energies and Power Quality (ICREPQ'26)
Santander (Spain), 10th to 12th June 2026
ISBN-13: 978-84-09-82044-3

Laboratory Characterisation of PMU-based Detection of Sub-Synchronous Oscillation

Stefano Lodetti[1], Frederick Wilkins[1], Peter Davis[1], Sahara Moshref[1], Paul Wright[1], Guglielmo Frigo[2], Deborah Ritzmann[1]

[1] National Physical Laboratory, Hampton Road, Teddington, United Kingdom
Corresponding author: stefano.lodetti@npl.co.uk

[2] Federal Institute of Metrology,
Bern, Switzerland

Abstract. This paper presents a laboratory study of the limitations and capabilities of sub-synchronous oscillations (SSOs) detection with a phasor measurement unit (PMU), with particular focus on amplitude attenuation. A test-bench to analyse the frequency response of a commercial PMU is presented, showing significant attenuation occurring outside the nominal system frequency range, which complicates the detection of SSOs. Experimental results demonstrate that while a PMU can detect SSOs under ideal conditions, attenuation and modulation effects can lead to misidentification or missed detections. The study highlights the need for advanced detection techniques and configurable PMU parameters to improve reliability in SSO monitoring.

Key words. small-signal stability, sub-synchronous oscillations, phasor measurement units, inverter-based resource, power system measurements

1. Introduction

The global transition towards net zero and the increasing integration of renewable energy sources are introducing new challenges to the operation and stability of power systems. Among these, power system oscillations have emerged as a critical concern due to their potential to signal instability and, if left unaddressed, lead to severe system-wide consequences [1]. Historically, oscillations in power systems were primarily associated with electromechanical interactions between synchronous generators and motors. However, recent developments have highlighted a new class of oscillations driven by the complex interactions among power electronic control systems [2]. These sub-synchronous oscillations (SSOs) are particularly relevant in systems with high penetration of inverter-based resources (IBRs), which are commonly used to connect renewable energy sources to the grid.

Monitoring and detecting SSOs is increasingly recognised as essential for maintaining system stability [3]. In grids with significant IBR integration, especially those with low system strength, SSO events have been reported with growing frequency. Notable examples include incidents in Texas (USA), China, Australia, and Great Britain. A comprehensive overview of real-world SSO events in such contexts is provided in [4], underscoring the urgency of developing reliable detection methods.

Currently, two main approaches are used to detect SSOs. The first involves post-event analysis using high-resolution digital fault recorders (DFRs), which offer high sampling rate and enable detailed characterisation of oscillatory behaviour. However, DFRs are not suitable for real-time detection, as data retrieval often requires manual intervention and on-site access.

The second approach uses phasor measurement units (PMUs) as specified in standard [5], which are increasingly deployed across transmission networks for wide-area monitoring. PMUs provide real-time synchrophasor data, allowing system operators to observe oscillatory behaviour and infer the presence of SSOs [6]. This is typically done by observing the amplitude of the oscillating phasor, or the value of the frequency of said oscillation despite their widespread use, PMUs were originally designed for protection applications in stable transmission systems where inverter-induced SSOs were not expected. The development in the signal processing mechanisms have made it possible to enhance the PMU accuracy and the capability to track fast dynamics, however this has not yet been reflected in an IEEE or IEC product standard. This leads to literature studies such as [7] to question their suitability for detecting and characterising SSOs. The work presented by the authors in [8] has demonstrated that PMU algorithms exhibit significant variability when measuring frequency components significantly below the nominal system frequency (50 Hz or 60 Hz).

The ability to measure SSOs is critical for understanding the dynamic behaviour of power systems under real-world operating conditions. Unlike traditional stability phenomena, SSOs often emerge unpredictably and can be influenced by subtle interactions among control systems, grid impedance, and converter configurations that are rarely reproduced in grid models. Without direct measurement, these oscillations may remain hidden, undermining system stability and limiting the effectiveness of preventive strategies. Equally important is the reliability of the measurement data itself. Instruments and sensors used to detect SSOs, such as PMUs, must be properly characterised and trusted to provide accurate information across the relevant frequency spectrum. Misleading or incomplete data can result in false conclusions, missed events, or inappropriate mitigation actions. As a result, there is a need to assess the capabilities and limitations of PMUs in detecting SSOs. Understanding what PMUs can reliably observe and where they may be blind is crucial for ensuring that system operators are not unknowingly missing critical oscillatory phenomena. This paper contributes to that effort by presenting a laboratory assessment of the performance of a class-M PMU in detecting SSOs and highlighting the implications for system monitoring and stability assessment.

2. Methodology

This section presents the laboratory test bench, test signals and SSOs characterisation methods that were utilised in the hardware-based evaluation of an off-the-shelf class-M PMU, aimed at identifying its limitations, capabilities, and blind spots in detecting SSOs.

A. Laboratory Test Bench

A laboratory test bench is configured to generate controlled signals containing oscillatory components. The setup includes a programmable power source capable of generating voltage waveforms with embedded SSOs. These signals are simultaneously measured by two isolated measurement devices. The first device is a class-M PMU, configured to record synchrophasors in real time. The PMU provides phasor estimation at 50 fps (frames per second), this is set for 50 Hz systems and, for simplicity, is configured to operate in single-phase mode. The second device is a waveform measurement unit (WMU), a high-resolution, high-speed digitising system, used to obtain a reference measurement. The WMU has an amplitude variation across frequency of less than 0.1 dB up to 30 kHz and is configured with a sampling rate of 50 kSa/s, measuring a signal to noise ratio of 58 dB on the fundamental. Fig. 1. illustrates the architecture of the test

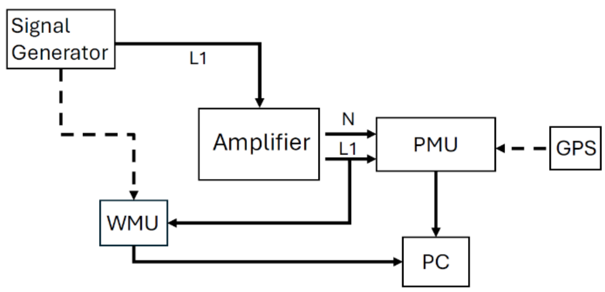

Fig. 1. Schematic of the laboratory test bench used for PMU evaluation. Key: Dashed line is a shared time signal, straight line is a shared electrical signal

bench.

The WMU provides raw voltage waveform samples from which SSO characteristics can be obtained directly without prior phasor estimation. Comparative analysis of the SSO characteristics obtained from PMU and WMU outputs enables assessment of any differences in detected oscillatory behaviour.

B. Test Waveforms

Based on a review of existing literature, key parameters were identified for characterising SSOs, including amplitude, frequency, start and stop time, rise time, and damping behaviour. The test signals are designed to reflect a range of variation of these parameters. The duration of each test signal was 30 s. Each test signal consists of an inter-harmonic component with variable amplitude and duration superimposed on a 50 Hz fundamental with constant 230 V amplitude, following the approach in [9] which demonstrated that the presence of an interharmonic component is both a necessary and sufficient condition for the existence of an oscillating phasor. Test waveforms are created with four amplitude envelopes:

1) Constant: interharmonic with constant amplitude.
2) Square: interharmonic amplitude is stepped up and down.
3) Triangle: interharmonic amplitude increases and decreases linearly.
4) Gaussian: envelope of interharmonic amplitude has a Gaussian distribution shape.

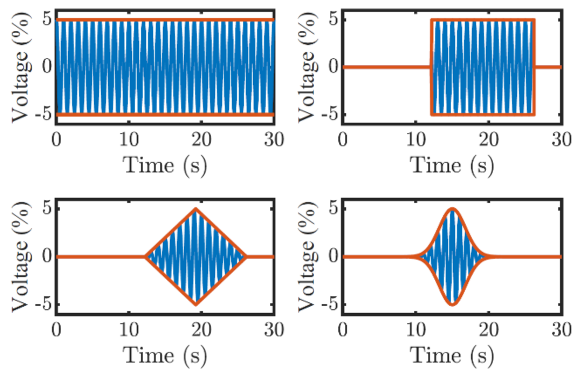

Fig. 2. Examples of amplitude modulation profiles used in the test signals: (a) constant, (b) square, (c) triangular, (d) Gaussian

The constant amplitude interharmonic is present for the full length of test signals, while the other envelope profiles have a shorter duration to emulate the start and end of an oscillation. Fig. 2. shows examples of the modulation profiles, and Table I summarises the test parameters including the amplitude and frequency values of the test SSOs.

Table I. – Parameters of Interharmonic Waveform Components

Envelope	SSO Test Parameters		
	Frequency range (Hz)	Amplitude (% of fundamental)	Duration (s)
Constant	5-65	0.1, 1, 2, 5, 10	Continuous
Square	5-60	1, 5, 10	14
Triangular	5-60	1, 5, 10	14
Gaussian	5-60	1, 5, 10	10.68

C. SSO Characterisation

To assess the response of measurement systems to SSOs, both amplitude and frequency of the SSO are extracted from the measurement results using a discrete Fourier transform (DFT). In the case of the PMU, the DFT is applied to the measured phasor amplitudes, while in the case of the WMU, spectral analysis is performed directly on measured waveform samples. In both cases a rectangular window is used. The SSO frequency is identified as the frequency component with the second highest amplitude since the frequency component with the highest amplitude is the fundamental.

For test signals with constant amplitude oscillations, a DFT window length of 24 s is used, discarding the first and final 3 s of the measured results to avoid edge effects. In modulated cases, a short-time Fourier transform (STFT) with a window length of 1 s is applied with 90 % overlap to track amplitude variation.

3. Results Of Constant Amplitude Tests

This section presents results aimed at characterising the range of SSO frequencies that can be identified with the PMU as well as the accuracy of identified SSO amplitudes at different frequencies. The procedure involved generating test signals with oscillation components at constant amplitude and frequency superimposed on the fundamental. The oscillation frequency is varied between test cases from 5 Hz – 65 Hz. All SSOs had an amplitude of 5 %. The test signals are measured with both the PMU and WMU devices and the SSO frequency was extracted in each case. The results effectively provide a characterisation of the bandwidth of the PMU, which is typically unknown or only specified within a narrow band of a few Hz around the nominal power system frequency (50 Hz in this work). It should be noted that, for the purpose of SSO analysis, characterisation is most relevant up to the system frequency of 50 Hz. Nevertheless, oscillations were tested up to 65 Hz to illustrate the symmetrical nature of the frequency response and to highlight potential aliasing effects beyond the typical operating range.

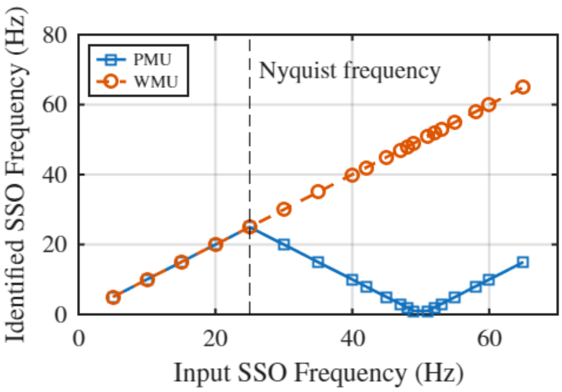

Fig. 3. Plot of the SSO frequency identified from the PMU and the WMU measurements compared to the generated SSO frequency

A. SSO Frequency

Fig. 3 shows a plot of the SSO frequencies identified from the PMU measurements and from the WMU measurements against signal input frequency of the oscillation which was varied from 5 Hz to 65 Hz. It can be seen that the reference obtained using the WMU system correctly captures the frequency of the SSO across the full range of interest. In contrast, the class-M PMU with a reporting rate of 50 fps accurately identifies the oscillation frequency only up to 25 Hz. For frequencies in the range 25 Hz – 50 Hz, the reported frequency corresponds to the difference between the actual oscillation frequency and the reporting rate of the PMU. This behaviour is a well-known limitation arising from the Nyquist theorem. As a result, an oscillation frequency identified to be 10 Hz from PMU data may correspond to a true mode at 10 Hz, 40 Hz, or even 60 Hz, due to repeated aliasing effects at higher frequencies, as shown in Fig. 3. This highlights the importance of understanding the bandwidth limitations of PMUs if their measurement results are used for SSO characterisation.

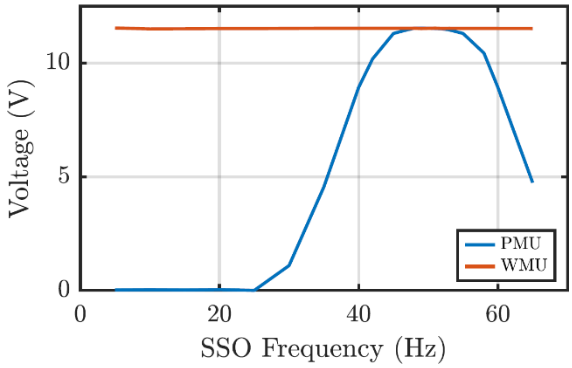

Fig. 4. Frequency response of the SSO amplitude showing the differences between the WMU and the commercial PMU. The input voltage of the SSO was 5% of the nominal voltage (230 V).

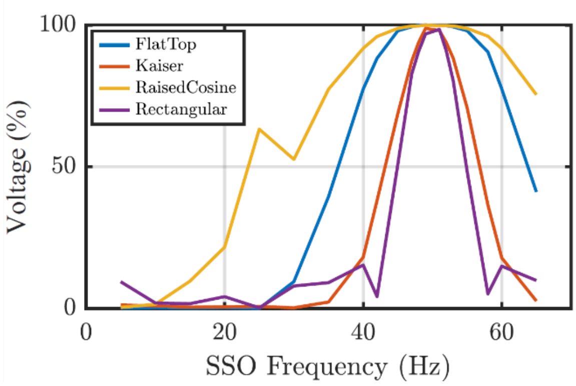

Fig. 5. Frequency response of a 5% amplitude SSO showing the differences between the available PMU window types, each having a 6-cycle window length

B. SSO Amplitude

Fig. 4 shows the frequency response of the SSO amplitude obtained from the PMU data, compared against the reference values obtained using the WMU data. As shown in Fig. 4, the frequency response of the PMU matches the WMU results only within a narrow band around the nominal system frequency of 50 Hz. Outside this band, the response decays steeply, resulting in significant attenuation. This behaviour is not surprising, as PMUs are designed to estimate the phasor accurately at 50 Hz, and any other frequency content is treated as noise and consequently rejected. This includes, for instance, harmonic distortion. However, this design choice complicates the detection of SSOs. In this case, it can be observed that the amplitude attenuation exceeds 50 % at approximately 15 Hz away from the system frequency. This is a critical consideration when utilising PMUs for SSO detection.

The observed attenuation is primarily attributable to the filter algorithm implemented in the PMU, and certain configuration options will mitigate this effect. The tested PMU supports modification of the windowing function and the number of power cycles used in the estimation process. Hence, the tests were repeated with various device settings to assess the impact on identified SSO amplitude. Fig. 5 illustrates the change in frequency response resulting from different windowing functions when the window length is 6 cycles, while Fig. 6 shows the effect of varying the number of cycles for the same window type (flat top). To facilitate the comparison, the figures present the PMU response as a percentage relative to the response of the WMU, which serves as the reference. All values are therefore normalised to 100 %.

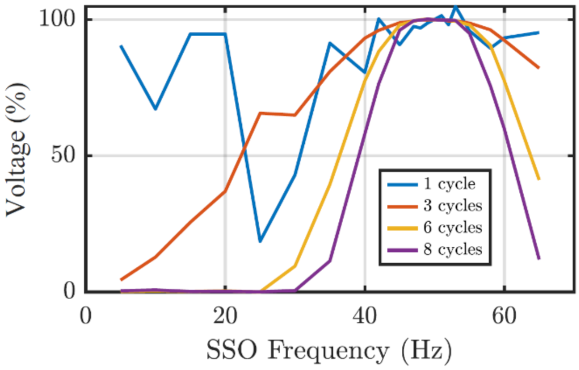

Fig. 6. Frequency response of a 5% amplitude SSO showing the differences obtained by varying the PMU window length for the Flat-Top filter window

It is important to note that the default configuration of the PMU is a flat-top window with six cycles, which corresponds to the setup used in Fig. 4. It can be seen how the choice of the window impacts the bandwidth of the PMU, with the raised cosine window being the one with the wider pass band and therefore, less attenuation of the SSO amplitude. Fig. 6 shows that reducing the number of cycles in the estimation algorithm can reduce the out-of-band attenuation, but it is also possible to observe instabilities when only one cycle is employed. This has shown to be particularly true for frequencies that are integer submultiples of the system frequency e.g., 25 Hz. The window choice is a trade-off between the mitigation of interference from off-nominal components and the responsiveness to grid dynamics. A one-cycle window would be fast in tracking grid dynamics but would equally result in many interharmonic component to be mapped into the fundamental estimate, making the PMU insufficiently accurate for class M. On the other hand, a longer window would make the step response too long to pass the step change test for class M [5]. Typical values for class M tend to be 4-6 cycles. The results from this section reinforce the importance of an accurate characterisation of the device when operated outside its intended range, and of the choice of measurement window depending on the intended application.

4. Results Of Amplitude Modulation Tests

This section presents comparative results for tests with time-varying oscillation signals since previous observations of real SSOs have shown dynamic behaviour that can grow or decay rapidly [4]. In the following plots, the amplitude values have been recentred around the peak for ease of comparison; the modulation envelopes used are those described in Section 2.B. Fig. 7 shows the SSO amplitude identified by the PMU and WMU for a square-modulated oscillation with input amplitude of 10 % and a frequency of 42 Hz. It can be observed that the SSO amplitude variation obtained from the PMU and WMU indicates the same oscillation duration, however, the amplitude obtained from PMU data is clearly lower than the amplitude obtained from the WMU data. This amplitude difference is expected considering the attenuation at 42 Hz observed in the frequency response analysis in the previous section.

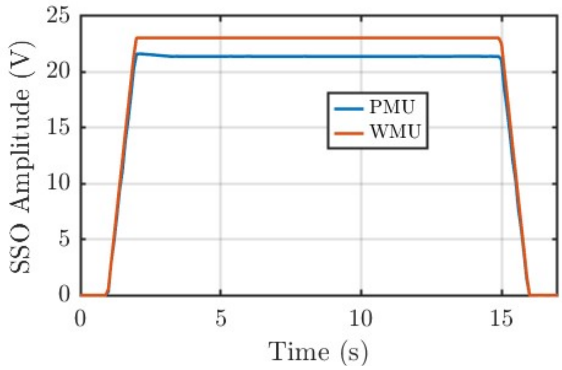

Fig. 7. Time characterization of SSO amplitude from the PMU and WMU with a 10 % SSO at 42 Hz.

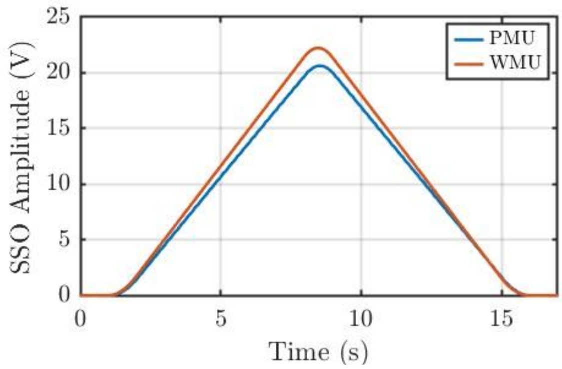

Fig. 8. Time characterisation of voltage signal from the PMU and a WMU with a 10 % SSO at 42 Hz with triangular modulation

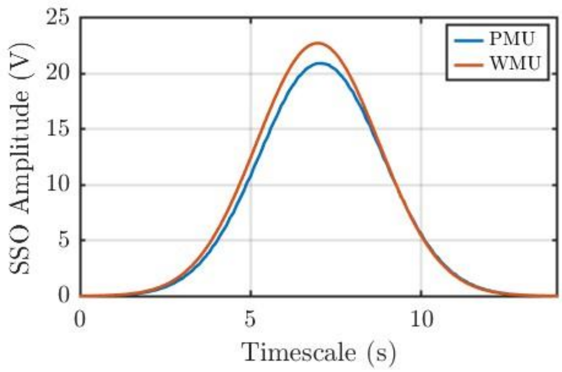

Fig. 9. Time characterisation of voltage signal from the PMU and a WMU with a 10 % SSO at 42 Hz with Gaussian modulation

Fig. 8 presents the results for an SSO with 10 % maximum amplitude at 42 Hz using triangular modulation, while Fig. 9 shows the same case with Gaussian modulation. In both cases the amplitude variation indicates a similar oscillation duration and the difference in amplitude obtained from PMU and WMU data scales with amplitude, with the PMU always underestimating the amplitude.

Fig. 10 shows the difference in SSO amplitude between PMU and WMU data for the square, triangular and Gaussian modulation cases; the differences is given as a percentage of the total input signal as measured by the WMU. The results show that the maximum difference in identified SSO amplitude is highest for the Gaussian modulation and in fact exceeds the difference obtained in the constant amplitude frequency sweep. On the other hand, in the case of the triangular modulation the maximum amplitude difference corresponds closely to the constant amplitude case, while the square modulation test results in a lower maximum amplitude difference. Initially these variations were surprising especially between the square modulated and constant cases as there were no differences in the experimental set up other than the duration of the SSO signal.

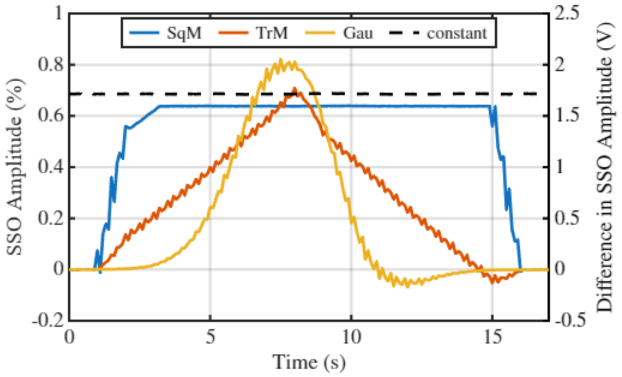

Fig. 10. Difference between the time characterisation of the SSO amplitude measured by the WMU and the PMU with a 10 % amplitude, 42 Hz SSO. Shown are the differences for the dynamic modulation and the constant SSOs as a percentage of the total input signal as measured by the WMU.

To trace the source of the variable differences between PMU and SSO measurements, a comparison was made between PMU measurements of the constant and flat top of the square modulated waveforms, and similarly between the WMU measurements. The comparison was made across the range of investigated frequencies. The results are shown in Fig.11. Across the frequency range the PMU measurements show a larger difference in the SSO amplitudes measured than the WMU measurements, with the largest difference being 0.44% of the total signal amplitude for the 40 Hz SSO. This suggests that the variations observed in Fig. 10 are due to the PMU measurements rather than the WMU or experimental setup.

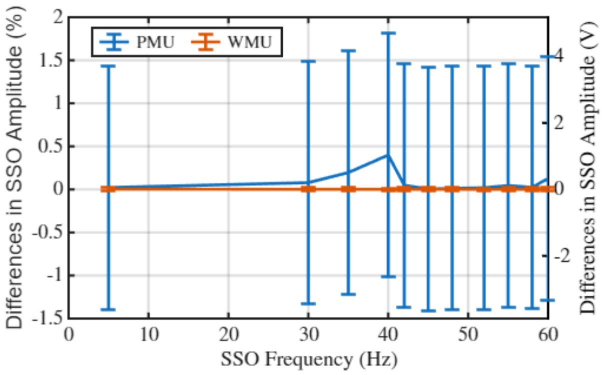

Fig. 11. Difference between the mean SSO amplitude measured in the square and constant modulations with a generated amplitude of 10 %, across a range of frequencies. Shown are the variation allowed in the phasor measurements whilst still complying with the C37.118.1-2011 standard for phasor measurements [10]

All the observed differences in the PMU measurements fall within the maximum total vector error of 1% specified in the standard for phasor measurements as visually represented by the error bars on Fig .11. [10]. Hence, the PMU is performing within requirements even at non-fundamental frequencies, however, the test results show that existing tolerances can lead to significant errors in measured SSO amplitudes.

In these scenarios, it can be observed that a simple threshold-based detector for SSOs may identify incorrect start and stop times or potentially fail to detect the oscillation altogether due to the variability allowed by the PMU standard, especially as SSOs in reality are often observed at lower amplitudes than the 10% used in these tests. Such cases necessitate adaptation of detection techniques to ensure adequate performance if PMU data is used for SSO detection.

5. Conclusions and Future Work

The objective of this work was to demonstrate the limitations of a generic class-M compliant PMU in the context of SSO detection, and to present a laboratory-based approach for performance characterisation. This is intended to support a more informed configuration of a measurement device for SSO detection and analysis applications. The presented results confirm that the limitations of PMUs, specifically their narrowband response centred around the system frequency, affect the accuracy of the identified SSO amplitude and frequency, particularly those located away from the system frequency or with modulated profiles. The results also underscore the effects of configurable PMU parameters, such as windowing function and cycle count. Additional signal processing options could enhance the PMU accuracy and the capability to track fast dynamics. The developed test bench provides a useful demonstration for characterising SSO monitoring equipment, including PMUs, prior to their deployment in the grid. This enables system operators to anticipate performance and limitations under realistic operating conditions. Future work should include the use of more realistic test waveforms, incorporating noise and distortion. This would allow for a more robust evaluation of detection algorithms and better reflect the challenges encountered in practical SSO monitoring scenarios.

Acknowledgement

This work was funded UK Government's Department for Science, Innovation & Technology through the UK's National Measurement System programme.

References

[1] L. Zhang, L. Harnefors and H. -P. Nee, "Power-Synchronization Control of Grid-Connected Voltage-Source Converters," in IEEE Transactions on Power Systems, vol. 25, no. 2, pp. 809-820, May 2010

[2] CIGRE JWG C4/B4.52, "CIGRE TB 909 - Guidelines for Subsynchronous Oscillation Studies in Power Electronics Dominated Power Systems," 2023.

[3] AEMO, “West Murray Zone Power System Oscillations 2020-2021 [report],” no. February, 2023.
[4] Y. Cheng, et al., “Real-World subsynchronous oscillation events in power grids with high penetrations of inverter-based resources,” IEEE Transactions on Power Systems, vol. 38, no. 1, 2023.
[5] “IEEE/IEC International Standard - Measuring relays and protection equipment - Part 118-1: Synchrophasor for power systems - Measurements,” in IEC/IEEE 60255-118-1:2018, vol., no., pp.1-78, 19 Dec. 2018
[6] H. Liu, et al., “Impacts of subsynchronous and supersynchronous frequency components on synchrophasor measurements,” Journal of Modern Power Systems and Clean Energy, vol. 4, no. 3, pp. 362–369, 2016.
[7] C. Wang, C. Mishra, K. D. Jones, R. M. Gardner, and L. Vanfretti, “Identifying Oscillations Injected by Inverter-Based Solar Energy Sources,” in IEEE Power and Energy Society General Meeting, 2022.
[8] S. Lodetti, et al., “Strategies and limitations for the detection of sub-synchronous oscillations in power systems” in conference on Renewable Energy and Power Quality (ICREPQ), Tenerife, Spain, 2025.
[9] W. Xu, J. Yong, H. J. Marquez and C. Li, “Interharmonic Power–A New Concept for Power System Oscillation Source Location,” in IEEE Transactions on Power Systems, vol. 40, no. 5, pp. 4367-4379, Sept. 2025.
[10] IEEE Standard for Synchrophasor Measurements for Power Systems," in *IEEE Std C37.118.1-2011 (Revision of IEEE Std C37.118-2005)* , vol., no., pp.1-61, 28 Dec. 2011, doi: 10.1109/IEEESTD.2011.6111219.